

Purposive Design of a Magnetic Sheet Metal Forming Facility

P. Werdelmann¹, D. Peier¹

¹ Institute of High Voltage Engineering and EMC, University of Dortmund, Germany

Abstract

This paper is about the identification of lumped elements within an electric circuit diagram in the context of electromagnetic sheet metal forming. Based on fundamental physical considerations the forming coil and its workpiece can be modeled as a transformer, which is loaded on its secondary side by a resistor. A systematic oriented design process relating to an aimed at purpose is introduced in order to avoid time extensive trial-and-error methods. Based upon the theory of electromagnetic field equations, the complex impedance of the sheet metal is analytically identified as a function of the radial component. Based on the introduction of a force equivalent quantity, ways of designing and optimizing the remaining free parameters are presented. Thus, a design process for a forming facility is possible as the desired electromagnetic force can be characterized by the currents running through the forming coil and the sheet metal.

Keywords:

Network synthesis, Analytic modeling, Electromagnetic coupling

1 Introduction

A purposive design of a magnetic sheet metal forming facility determines the properties of the needed elements, apart from already existing realizations, under the aspect of efficiency and robustness. To assess the result of such a design process, it is important to know the principal restrictions, which are given by the forming mechanism itself and various boundary conditions. The following chapters examine the general behaviour of the magnetic forming process by use of an electric network model. The objective which is to be examined is the temporal distribution of the electromagnetic force the workpiece is exposed to. Therefore, a description of the aerielly distributed force density is captured by means of an equivalent quantity, which is expressed by integral values within the electric circuit structure.

2 Equivalent circuit structure

The main principle of an electromagnetic sheet metal forming process is the interaction between a generated magnetic field and induced eddy currents resulting in electromagnetic force. Figure 1 shows the arrangement consisting of a flat spiral coil beneath a conducting plate. A pulsed current $i_1(t)$ through the forming coil causes a temporally changing magnetic flux Φ_1 , which affects the sheet metal diffusely and induces an eddy current $i_2(t)$ within the workpiece. Obviously, this coupling of two currents by a magnetic field shows analogy to a transformer concerning the ability of being modeled by an electric circuit diagram.

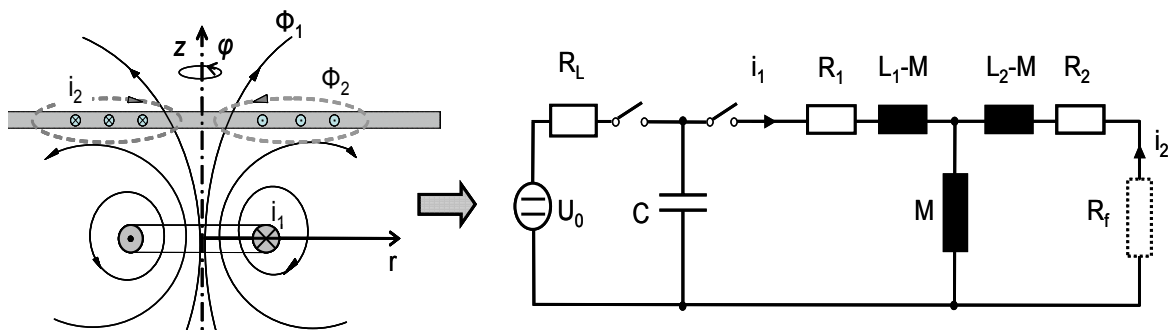


Figure 1: Principal structure of an electromagnetic sheet metal forming facility. The setup consisting of a flat spiral coil beneath the workpiece is modeled by the equivalent circuit diagram of a transformer

The primary side of this electric network model describes the forming tool with its self-inductance L_1 in series with an ohmic resistance R_1 . By means of the mutual inductance M the coil current is coupled with the workpiece current density, which is aurally distributed within the sheet metal. Its network elements R_2 and L_2 depend on the material's conductivity as well as on the frequency. The secondary side of this transformer is loaded by another resistive element R_f , which dissipates the forming energy being transferred to the workpiece. This energy is part of the initially stored energy provided by the capacitive energy storage C . Further research activities, which have not been published yet, reveal that the current through the workpiece is barely affected by the resistance R_f so that the resistance R_2 is assumed to be much larger than R_f . This assumption is valid for a fixed sheet metal or if the workpiece is activated by a short initial impulse of force.

The transition from aurally distributed quantities to concentrated network elements has to keep a physical reasonability as the magnetic flux is modeled by the network structure's inductivities relating to the respective flux causing current. These, of course, are integral values; hence, the electric circuit diagram in figure 1 can not directly consider any densities or spatial electromagnetic field distributions.

3 The sheet metal's network elements

The equivalent lumped elements R_2 and L_2 of the workpiece are determined by a given local distribution of the current i_2 , which is based on the induction of an eddy current density $J_2(t)$ at a certain frequency. The complex impedance of a metallic conductor is generally given as the quotient of the electric voltage and the current. In case of presence of the skin effect there is no homogeneous current density within the conductor's cross section. Thus, with regard to figure 2, the resulting complex impedance is being expressed with respect to the causing field quantities [1, 2]. In case of a rotationally symmetric conducting plate the impedance is formed by the circumferential electric field strength E_0 at the plate's surface in relation to the entire current flowing through the workpiece.

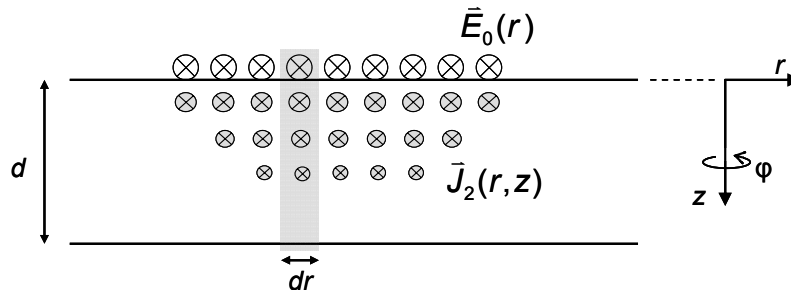


Figure 2: Simplified illustration for the determination of the sheet metal's complex impedance. Within an infinitesimal cross section the field distribution is homogeneous

$$\underline{Z} = \frac{\underline{U}}{\underline{I}} = \frac{\oint \bar{E}_0(r) dl}{\iint \bar{J}_2(r, z) dr dz} \quad (1)$$

This equation is valid for homogenous field distribution among the radius. However, $E_0(r)$ and $J_2(r, z)$ are functions depending on the r - and z -component. The z -dependence is known and can be separated as a factor, which is not possible for the radial dependence. Thus, impedance per unit length remains instead of a discrete value from equation (1) when integrating the current density among the plates thickness d . The resulting impedance per unit length can thereby be written as a function of the radius and depends on the frequency, as considered by the skin penetration depth δ [3].

$$\underline{Z}'(r) = \frac{2\pi r \cdot \bar{J}_0(r)}{\kappa \cdot \bar{J}_0(r) \cdot \int_0^d e^{-\frac{(1+j)z}{\delta}} dz} = \frac{2\pi r \cdot (1+j)}{\kappa \cdot \delta \cdot \left[1 - e^{-\frac{(1+j)d}{\delta}} \right]} \quad (2)$$

To get an expression for concentrated network elements, the complex apparent power \underline{S}_2 can be calculated as an integral value. The real part of this expression represents the real power, which is dissipated by the ohmic resistance R_2 , whereas the imaginary part

corresponds with the idle power and the plate's inductance L_2 . For an assumed current distribution these quantities are presented in figure 3 as functions of the frequency. When relating the real part of the sheet metal's impedance R_2 to the imaginary part ωL_2 it can be seen that there is a global minimum of the impedance relation, depending on a certain frequency.

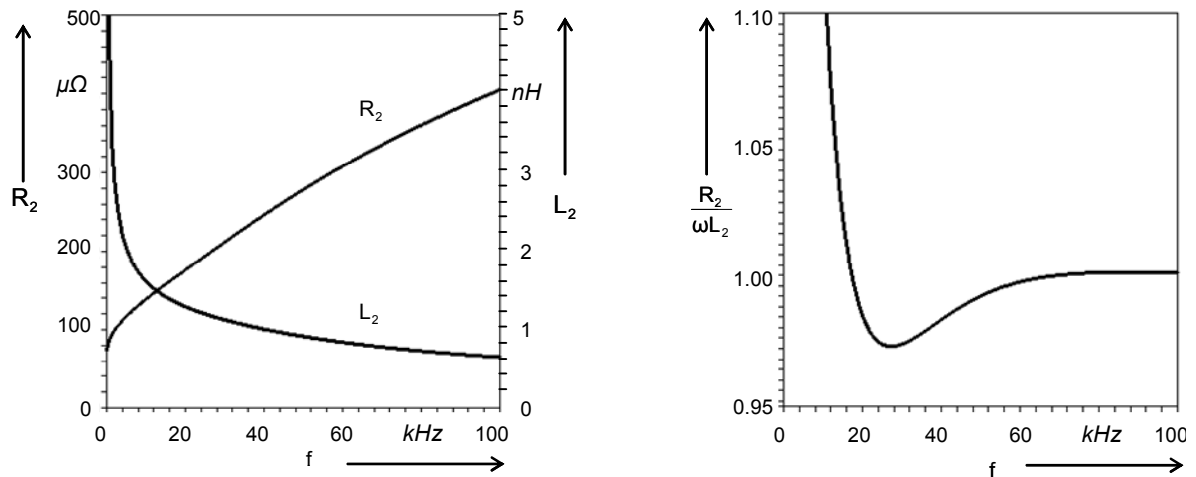


Figure 3: Course of the sheet metal's resistance R_2 and inductance L_2 and the relation of both as a function of the eddy current's frequency (material: aluminium, $d=2\text{mm}$)

4 Calculation of the electromagnetic force

By means of field quantities the resulting electromagnetic force between forming coil and workpiece is obtained by the vector product of the coil's magnetic flux density B_1 and the eddy current density J_2 within the workpiece [4]:

$$\vec{F} = \vec{J}_2 \times \vec{B}_1 \quad (3)$$

Regarding the electric circuit structure from figure 1, J_2 is expressed by the integral quantity $i_2(t)$, whereas B_1 is represented by the product of the coil's self inductance L_1 and the flux causing current $i_1(t)$. Therefore, a substitutive quantity as an equivalent $F^*(t)$ for the magnetic force $F(t)$ is given by equation (4).

$$F(t) \sim L_1 \cdot i_1(t) \cdot i_2(t) = F^*(t) \quad (4)$$

By this expression it is evident that the whole information about the temporal development of the electromagnetic force can be obtained from the electric equivalent circuit diagram.

For a further discussion the elements from the circuit structure in figure 1 are lumped to substitutive elements, which provide the ability of the transition to a RLC series resonant circuit. These elements are determined by rules of network calculation and are carried over to a substitutive network topology, as shown in figure 4.

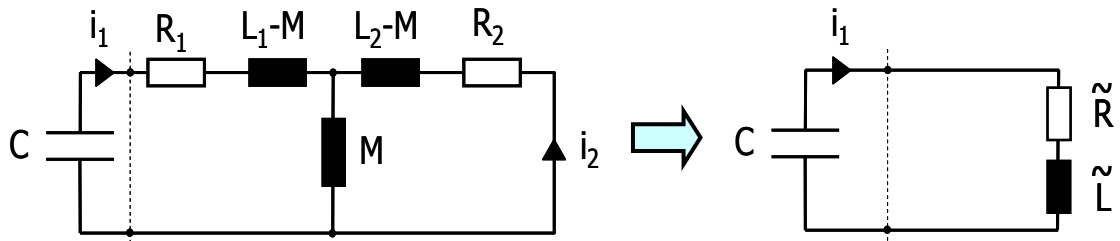


Figure 4: Transition from a transformer equivalent circuit to a RLC series oscillating circuit

$$\tilde{R} = R_1 + \frac{R_2 \cdot \frac{M^2}{L^2}}{1 + \left(\frac{R_2}{\omega L_2}\right)^2} \quad \text{and} \quad \tilde{L} = L_1 - \frac{L_2 \cdot \frac{M^2}{L^2}}{1 + \left(\frac{R_2}{\omega L_2}\right)^2} \quad (5)$$

The new circuit diagram's damped oscillation is characterized by the resonant angular frequency ω_0 and the quality factor Q [5,6], as expressed by equation (6).

$$\omega_0 = \frac{1}{\sqrt{\tilde{L}C}} \quad \text{and} \quad Q = \frac{\sqrt{\tilde{L}C}}{\tilde{R}} \quad (6)$$

For the RLC series oscillation circuit an ordinary second order differential equation for the capacitor's voltage is obtained due to the fact that there are two different types of energy stores in this network. The corresponding solution for the coil current is found to be:

$$i_1(t) = -\omega \cdot C \cdot U_0 \cdot \frac{4Q^2}{4Q^2 - 1} \cdot e^{\left(-\sqrt{\frac{1}{4Q^2 - 1}} \cdot \omega t\right)} \cdot \sin(\omega t) \quad (7)$$

The identified coil current is subsequently used to determine a mathematical expression for the load current $i_2(t)$ flowing through the sheet metal. Within the electric circuit diagram in figure 4, the load branch is parallel to the mutual inductivity so that the voltages may be equated, resulting in a first order differential equation for the coil current $i_2(t)$, for which the solution is given in equation (8). Within this expression, a phase shift ψ occurs, which is mainly caused by the sheet metal's parameters R_2 and L_2 , as expressed by equation (9).

$$i_2(t) = -C \cdot U_0 \cdot \frac{M}{L_2} \cdot \frac{\sqrt[3]{\frac{4Q^2}{4Q^2 - 1}}}{\left(1 + \left(\frac{1}{\sqrt{4Q^2 - 1}} - \frac{R_2}{\omega L_2}\right)^2\right)} \cdot \left[\sqrt{1 + \left(\frac{1}{\sqrt{4Q^2 - 1}} - \frac{R_2}{\omega L_2}\right)^2} \cdot e^{\left(\frac{\omega t}{\sqrt{4Q^2 - 1}}\right)} \cdot \sin(\omega t + \psi) - \frac{R_2}{\omega L_2} \cdot e^{\left(\frac{R_2 \cdot \omega t}{\omega L_2}\right)} \right] \quad (8)$$

$$\psi = \arctan \left(\frac{\frac{R_2}{\omega L_2}}{1 - \frac{1}{1-4Q^2} - \frac{1}{\sqrt{1-4Q^2}} \cdot \frac{R_2}{\omega L_2}} \right) \quad (9)$$

The expression for the workpiece current $i_2(t)$ shows the same exponentially damped, sinusoidal temporal development as the coil current $i_1(t)$. In addition, the sheet metal's network parameters cause a volatile current component, which causes an extra damping of the current's first amplitude peaks. Because of the phase shift ψ the product of both currents is not always positive, which leads to a possible change of the force's direction. Figure 5 shows the run of the force equivalent quantity F^* for a workpiece constant of $R_2/\omega L_2=1$ as a function of time and the quality factor Q .

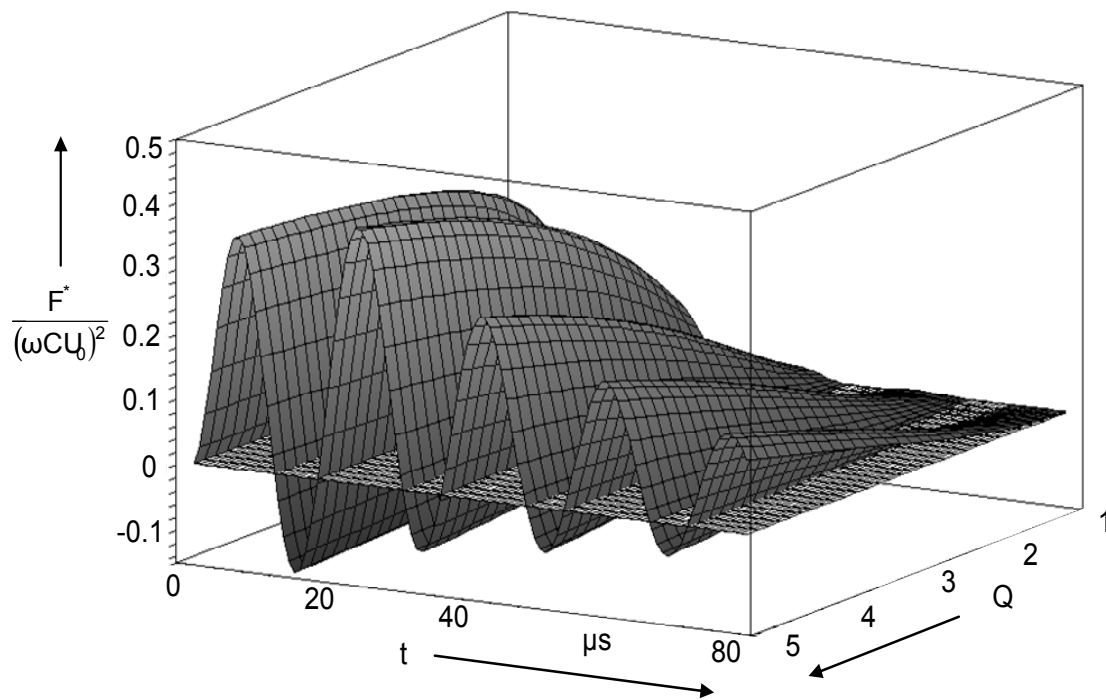


Figure 5: Normalized temporal development of the force equivalent quantity F^* , depending on the facility's quality factor. For a certain workpiece constant ($R_2/\omega L_2=1$) a negative force is possible due to the phase shift between the participated currents, and thus, decreasing the efficiency

5 Assessment of the forming process

For the best temporal course of an initial electromagnetic force, trying to get near a desired unipolar temporal course, the argument of the arctan function in equation (9) has to be minimized. This is achieved for a high quality factor Q as well as for a small workpiece constant $R_2/\omega L_2$. For a purposive analytical design strategy the challenge is to determine the free parameters of an existing forming facility in order to match the required demands. For typical applications and types of workpiece materials the workpiece parameter $R_2/\omega L_2$ is almost equal to 1, as figure 3 reveals. With this constant, expressions (5) can be simplified and put into the quality factor's equation (6). By introducing the magnetic leakage factor σ a conditional equation for the overall Q -factor is obtained in equation (10).

$$Q = Q_A \cdot \frac{\sqrt{\frac{\sigma+1}{2}}}{1 + \frac{1}{2} \cdot \frac{L_1}{R_1} \cdot \frac{R_2}{L_2} \cdot (1-\sigma)} \quad \text{with } \sigma = 1 - \frac{M^2}{L_1 \cdot L_2} \quad (10)$$

Q_A is the quality factor and ω_{0A} the resonant angular frequency of the facility in non-load operation, e.g. without the workpiece.

$$Q_A = \frac{1}{R_1 \cdot C \cdot \omega_{0A}} \quad \text{with } \omega_{0A} = \omega_0 \cdot \sqrt{\frac{\sigma+1}{2}} \quad (11)$$

The proportion R_1/L_1 in equation (10) is obtained by the combination of (5), (6), and the magnetic leakage factor σ .

$$\frac{R_1}{L_1} = \frac{1}{2} \left(\frac{\omega_0}{Q} (\sigma+1) + \frac{R_2}{L_2} (\sigma-1) \right) \quad (12)$$

These general expressions imply the needed information for the application of a design process. From section 3 the sheet metal's impedance is received for the postulation that the skin penetration depth δ matches a quarter of the plate's thickness d , which implies a required frequency f . This assumption is made on the condition that, the magnetic field should be properly shielded by the workpiece. Generally, the skin penetration depth is user-defined and can be chosen. The quality factor is determined to be a value for which there is no more gain of the force equivalent's magnitude to be expected for an increasing Q . The according parameters are listed in table 1.

d [mm]	δ [mm]	f [kHz]	R_2 [$\mu\Omega$]	L_2 [nH]	$R_2/\omega L_2$	Q
2.0	0.5	28.14	209	1.22	0.973	3.5

Table 1: Design specifications and the resulting sheet metal parameters for a chosen skin penetration depth of $\delta=d/4$

To show the interrelation of the respective quantities, a graphic interpretation is presented in the form of a nomogram. Figure 6 pictures the nomogram of equations (10)-(12) for a specific workpiece parameter $R_2/\omega L_2=0.973$.

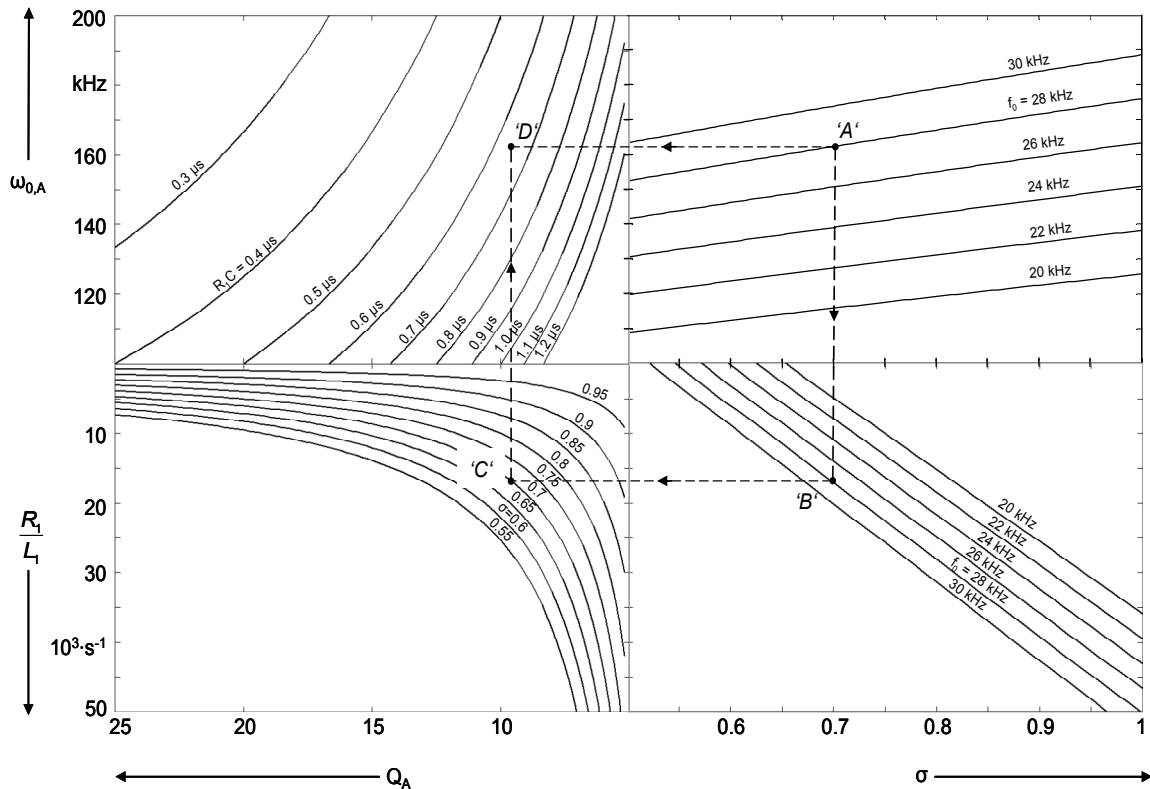


Figure 6: Nomogram chart of the mathematical relation of the participated quantities to identify the optimal combination of the facility's parameters

Each equation has its own pair of axes, implicating that particularly two quadrants share one common axis. The first quadrant shows the resonant angular frequency ω_{0A} over the leakage factor σ of the non-loaded facility with the frequency f_0 of the entire set, acting as the parameter for the array of curves. The second quadrant pictures the curves of the facility's quality factor Q_A as a function of its resonant frequency ω_{0A} . The parameter for these curves is the capacitor's time constant R_1C . Additionally, this quality factor is shown as a function of the reciprocal coil's time constant R_1/L_1 . According to equation (12), the fourth quadrant shows the quantity R_1/L_1 , depending on the magnetic leakage factor σ with the resonant frequency f_0 as parameter. The leakage factor σ is a rate for the magnetic coupling between forming coil and workpiece. It should be mentioned that all scales within this chart are suppressed-zero scales. So it is evident that there are definite restrictions concerning a technical feasibility.

With the parameters from table 1, which act as input data for the optimization, an example design process is performed with the objective to identify the optimal coil parameters regarding to a given energy store. For this arrangement the influence of a different leakage factor as a rate for a changing mutual inductance is parametrically

examined. The starting information is the leakage factor σ for which, in combination with the given frequency $\omega \approx \omega_0$, the point 'A' is determined. A projection into the fourth quadrant delivers the point of intersection with the same parameter's curve in 'B'. Keeping in mind the start information σ , the only curve to be depicted out of the array in quadrant three is the one for the same leakage factor as parameter. Point 'C' is projected into the second quadrant where the intersection with the determined resonant frequency ω_{0A} reveals the conditional value for the time constant R_1C . In combination with equations (10) to (12) the unknown elements can be identified. In table 2 the identified network elements of the forming coil are listed for three different cases of an initial leakage factor, from which the third case's path ('A-B-C-D') is pictured exemplarily in the nomogram chart. The boundary condition for this example is formed by the capacity, which is set to $C = 10 \mu\text{F}$.

	R_1/L_1	Q_A	ω_{0A} [kHz]	f_{0A} [kHz]	R_1C [μs]	R_1 [m Ω]	L_1 [μH]	M [nH]
$\sigma=0.60$	6 500	25.0	157	25.0	0.27	27	0.42	15.5
$\sigma=0.65$	12 000	13.5	160	25.5	0.46	46	3.84	43.7
$\sigma=0.70$	17 000	9.5	162	25.8	0.65	65	3.82	40.34

Table 2: Solution of the forming coil's optimized parameters for the load parameters given in table 1

For different values of the leakage factor the quality factor of the facility gets smaller, whereas the relation between ohmic resistance and self-inductance R_1/L_1 of the forming coil has to be increased in order to keep the main quality factor Q high and the phase shift ψ low.

6 Conclusion and outlook

Within this work, ways of identifying and optimizing unknown network elements of an electromagnetic forming facility's components are presented. In order to set up conditional equations for the examined quantities, the temporal behaviour of the entire facility is investigated by means of electric network analysis. Thus, the coil current as well as the workpiece current are obtained as solutions of the system's particular ordinary differential equations. As the one-dimensional network model can not consider any aerial distributions of electromagnetic field terms, a substitutive quantity for the electromagnetic force as an integral value is introduced. Therefore, the product of the coil's self-inductance with both the coil's current and the work piece's current, is examined and treated as the objective function, for which an optimal time course is aimed at.

Due to a phase shift between coil and workpiece current the resulting force changes its direction momentarily, which is dependent on the workpiece characteristic.

The sheet metal's concentrated network elements are obtained by treating the apparent power within the sheet metal as an integral value, which is caused by the aerielly distributed eddy current density and the radial impedance per unit length. The influence of different materials acting as the workpiece regarding the efficiency of electromagnetic sheet metal forming can be examined in terms of the system's network performance. The mentioned phase shift is treated to be minimized, but the time-based analysis of the electric network model reveals that this phase angle will only disappear if the workpiece's resistive part tends to zero. This implies that an entirely unipolar temporal development of the electromagnetic force can not be achieved.

The quality factor of the entire system has been shown to be a useful criterion for optimizing the process' efficiency. Therefore, the mathematical interrelations between the participating quantities is figured out and used to determine the system's free parameters. The presentation of the individual functions, which are affecting the quality factor, is useful to get an overview of the respective coherences. This chart also shows restrictions for the range of the optimized quantities, according to a technical feasibility.

The presented design process can also be applied backwards with only little change in operation for different demands. For example, this will be useful to determine the optimal set of parameters for diverse types of energy stores, whether it is a capacitive or inductive one. Having determined a set of optimized electrical network parameters, the next step should be to apply this information to a geometric design process concerning the magnetic field distribution with regards to geometry.

References

- [1] *Simonyi, K.:* Theoretische Elektrotechnik. Barth Verlagsgesellschaft, Bad Langensalza
- [2] *Schunk, H.:* Stromverdrängung. Dr. Alfred Hüthig Verlag, Heidelberg, p. 104-108, 1973
- [3] *Binns, K.J.; Lawrenson, P.J.; Trowbridge, C.W.:* The Analytical and Numerical Solution of Electric and Magnetic Fields. John Wiley & Sons Ltd, Chichester, p 97-99, 1992
- [4] *Schmidt, V.:* Untersuchung der magnetischen Induktion, Stromdichte und Kraftwirkung bei der Magnetumformung. Verlag W. Girardet, Essen, p. 35, 1976
- [5] *Philippow, E.:* Taschenbuch der Elektrotechnik, Band 1. Carl Hanser Verlag, München, 1976
- [6] *Leonhardt, W.:* Wechselströme und Netzwerke. Vieweg Akademische Verlagsgesellschaft, Braunschweig, 1968